Study on the splitting failure of the surrounding rock of underground caverns

Xiaojing Li[1], Han-Mei Chen[*2], Yanbo Sun[3], Rongxin Zhou[4], Lige Wang[4]

[1]*Department of Civil Engineering, Shandong Jianzhu University, Jinan, 250101, China*
[2]*NewRail Centre for Railway Research, Newcastle University, NE1 7RU, UK*
[3]*Shandong Luqiao Group CO,.LTD, 250101, China*
[4]*Institute for Infrastructure and Environment, School of Engineering, The University of Edinburgh, EH9 3JL, UK*

(Received keep as blank , Revised keep as blank , Accepted keep as blank)

Abstract. In this paper splitting failure on rock pillars among the underground caverns has been studied. The damaged structure is considered to be thin plates and then the failure mechanism of rock pillars has been studied consequently. The critical load of buckling failure of the rock plate has also been obtained. Furthermore, with a combination of the basic energy dissipation principle, generalized formulas in estimating the number of splitting cracks and in predicting the maximum deflection of thin plate have been proposed. The splitting criterion and the mechanical model proposed in this paper are finally verified with numerical calculations in FLAC 3D.

Keywords: splitting failure, deflection, surrounding rock, underground caverns, crack prediction

1. Introduction

With the carrying out of 'West China Development Strategy', various civil projects are booming in western China where a lot of underground constructions are ongoing or will be undertaken. Most of these projects are characterized with deep embedment. While excavating underground caverns under high in-situ stresses, longitudinal splitting cracks are apt to appear on the brittle surrounding rock. It would induce parallel large splitting fissures, following by intense brittle deformation and failure, such as rock burst, which seriously endanger the stability and the safety of the caverns. Take the project of Ertan Hydropower Station in China as an example, the release and redistribution of high horizontal in-situ stresses resulted in several serious splitting cracks on the sidewalls of main plant,. And the depth of cracks was reported to be more than 20 m. This similar phenomenon was observed in many projects in China.

Hibino and Motojma (1995) investigated 16 large Japanese underground powerhouses. Based on their statistical results the crack opening or expansion phenomenon happened in most of the powerhouses within a certain range. Therefore it can be stated that this kind of cracking occupied a large proportion of deformation and failure. A number of studies on failure criterion of the surrounding rock have been conducted during these years, e.g. the stability classification method of surrounding rock, the stress criterion based on strength, the critical strain or displacement

∗Corresponding author, Ph.D., E-mail: maggie_chen007@hotmail.com

criterion based on deformation (Chatterjee *et al*. 2015) and the method of displacement rate discrimination (Li *et al*. 2015) etc.

Nomenclature

γ	Unit weight
c	Cohesion
μ	Poisson's ratio of the rock for the Ertan Hydropower Station
φ	Friction angle
ν , $\bar{\nu}$	Poisson's ratio before and after the failure of the rock unit, respectively
E , $\bar{E}$	Modulus of deformation before and after the failure of the rock unit, respectively
N_x, N_y, N_z	Axial force in X, Y, Z direction, respectively
W_s	The energy released at critical state
ε_{cr}	The critical buckling strain
σ_t	Tensile strength of rock
σ_{cr}	The critical buckling stress
$\sigma_x, \sigma_y, \sigma_z$	The main principal stresses of the unit before failure
$\sigma_x^*, \sigma_y^*, \sigma_z^*$	The main principal stresses of the unit during failure

Among these methods, the strength and displacement criterion are the most two common approaches and they are actually complementary to each other (Wong and Einstein 2009, Wu and Wong 2012). Strength analysis and corresponding strength criterion play a crucial role on understanding the failure mechanisms of surrounding rock, the phenomenon of strength failure and designing supports (Xue 2015, Panaghi *et al*. 2015, Zhu *et al*. 2014). However, the criterion for splitting failure was reported rarely. When cavern sidewalls with micro-cracks are under high in-situ stresses, the small fissures on them can then expand to parallel large splitting fissures, such that the methods for studying the internal cracks of rocks are no longer applicable. A more suitable model of rock mechanics has to be developed to correctly present splitting fissures and failure of the surrounding rock. (Li *et al*. 2014, Altindag and Guney 2011, Song *et al*. 2015)

According to the results of model tests, the internal deformation of the surrounding rock of underground excavation with high walls is not continuous under high in-situ stresses; instead the cracking and plate cracking can be observed on the surrounding rock under tangential force. Subsequently, under the axial force and gravity, the bending deformation happens on the plate strips which are formed after plate cracking. The bending deformation is dependent on the strip length and cross-sectional dimension. (Wang *et al*. 2016, Hoek and Martin 2014, Jiang and Feng 2011, Huang *et al*. 2013, Lajtai *et al*. 1991, Liolios and Exadaktylos 2013, Maheshwari 2009, Martin *et al*. 2013)

In this paper an in-depth study of the splitting failure of the surrounding rock of Ertan underground caverns has been extensively conducted with the basic principles of energy dissipation combining with plate buckling theory and numerical calculations. Furthermore, a generalized prediction model of splitting cracks and a formula which can calculate the maximum deflection of thin plate have been proposed and further verified in the Ertan project.

2. Analysis of the basic principle of splitting failure by using energy method

It is well known that before excavation, the surrounding rock of the underground caverns is in three-dimensional stresses, which maintains the caverns under equilibrium state. After excavation, there are loading and unloading zones in the surrounding rock in which the rock is in elastic state. Thus the internal system is in a uniform deformation state without macroscopic irreversible process. (Palchik and Hatzor 2002, Ruffolo and Shakoor 2009)

The rock excavation system of the underground cavern is an open system, such that the rock unit could exchange energy with its exterior and then causes stress accumulation. During this process, some rock units may accumulate excessive stress at the stage of rupture development. Once the stress exceeds the elastic limit, the rock is under plastic deformation such that micro-cracks begin to appear in the surrounding rock, and micro-cracks will be under constantly progressive development with the increase of stress difference. For the rock within the loading zone, stress concentration has a significant increase and rock fracture zones appear locally with continuous and progressive development. When the stress redistribution reaches a certain level, it will produce a motion form which can then dissipate energy, such as the plastic energy dissipation due to the plastic deformation of rocks and the fracture energy dissipation due to the tensile failure of rock.

3. Theoretical study on the thin plate buckling for the instability of rock pillar

3.1 The applicability test of the thin plate model

In elastic mechanics, there are specific conditions for the calculation of beams, plates, cylinders etc. The plates, in fact, refer to the moderately thick plates. The ratio of the thickness of the plate to the minimum board thickness min (a, b) is from 1/100 to 1/3. For rock material, its greatest feature is that the tensile strength is far less than the shear strength; the shear strength is less than the compressive strength. Thus, the strength of the rock is substantially controlled by uniaxial tensile strength. The maximum tensile stress is the main cause of rock mass destruction. For hard brittle rock, the feature is more obvious. Therefore, the geometrical condition which defines the rock slab as a thin plate can be relaxed appropriately.

Sanchidrian *et al*. (2012) stated that the thin plate method can be also applied in the study of the rock slab when t/b is no more than 1/3. However; when t/b is more than 1/3, the thin plate method may not be suitable anymore; instead the plate should be treated as thicker plate. Thus the geometrical conditions of the rock slab in present study totally satisfy the thin plate assumption. Furthermore, the deflection of the rock slab itself is no greater than the thickness of the slab, which is consistent with the prerequisite of the small deflection theory of thin plate bending. Hence, in order to study the splitting cracks of the brittle surrounding rock wall of caverns and the failure mechanism under high in-situ stresses, it is appropriate to select the thin plate mechanical model in this paper.

3.2 Problem statement

When the plate is under longitudinal load at the border, a certain in-plate force will occur. In order to make the plate maintain in any bending state, it is necessary to impose a lateral disturbing

force. After the disturbing force is removed, the plate can restore to the original equilibrium state via a vibration process.

However, if the in-plate force in some parts or some directions caused by longitudinal load is compressive force, the equilibrium state will be unstable when longitudinal load exceeds a certain value (threshold value). The phenomenon that thin plate in a bent state of equilibrium under longitudinal load is known as buckling.

The plate buckling differential equation can be given as (Sofianos *et al*. 2014):

$$D\nabla^4 \mathrm{w}\text{-}(\mathrm{N_y}\frac{\partial^2 w}{\partial y^2}+2\mathrm{N_{yz}}\frac{\partial^2 w}{\partial y\partial z}+\mathrm{N_z}\frac{\partial^2 w}{\partial z^2})=0 \tag{1}$$

This is the homogeneous differential equation of the deflection w, in which the coefficients $N_{\mathrm{x}}, N_{\mathrm{y}}, N_{\mathrm{xy}}$ are represented by the longitudinal load with already known distribution but unknown value.

3.3 Critical load of the thin plate buckling

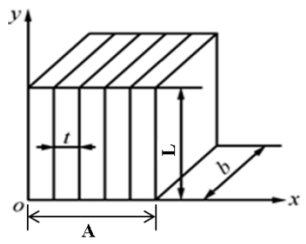

(a)

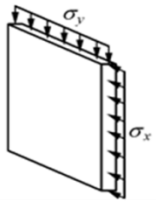

(b)

(c)

Fig. 1 The sketch of thin plate buckling

Since splitting cracks at the cavern wall has been equivalent to plate buckling as stated above, the mechanical model can be simplified to a specific model in which two sides are clamped and supported, while the other two are free. Thus we have the boundary conditions: $N_y=-N$, $N_z=0$, $N_{yz}=0$, after substituting them into Eq. (1), the following equation can be obtained:

$$D\nabla^4\omega+\mathrm{N_z}\frac{\partial^2 w}{\partial z^2}+\mathrm{N_y}\frac{\partial^2 w}{\partial y^2}=0 \tag{2}$$

Deflection equation of the model can be written as (Chinnasane 2004, Tang 2004):

$$\omega(y,z)=\xi\left(1-\cos\frac{2\pi y}{L}\right)\left(1-\cos\frac{2\pi z}{b}\right) \tag{3}$$

Where $\xi=\frac{\sigma_t t}{6\sigma_{cr}}$, σ_t is the tensile strength of rock.

The boundary condition of the thin plate is $u\Big|_{\left(y=\frac{L/2}{-L/2}\right)}=0$, $\frac{\partial w}{\partial y}\Big|_{\left(y=\frac{L/2}{-L/2}\right)}=0$, $u\Big|_{\left(z=\frac{b/2}{-b/2}\right)}=0$, $\frac{\partial w}{\partial z}\Big|_{\left(z=\frac{b/2}{-b/2}\right)}=0$.

After computing, the critical buckling stress value can be calculated,

$$\sigma_{cr}=\frac{\pi^2 Et^2}{3L^2} \tag{4}$$

When the plate reaches a critical strength value at failure, the energy released at critical state is,

$$W_s=\frac{1}{2}\int_{-0.5b}^{0.5b}\int_{-0.5L}^{0.5L}\sigma_{cr}\left(\frac{\partial\omega}{\partial y}\right)^2\left(\frac{\partial\omega}{\partial z}\right)^2 dydz=\frac{\pi Ebt^4\sigma_t}{36L^2\sigma_{cr}} \tag{5}$$

This energy expression has a relationship with the tensile strength of the surrounding rock and the compressive strength of the thin plate, which can well reflect the energy change of the thin plate splitting cracks, forming in the internal of the surrounding rock.

3.4 Energy dissipation analysis of the plate buckling

In energy dissipation analysis of the plate buckling, the uneven stress distribution caused by excavation is ignored in order to qualitatively describe the splitting failure near the cavern. Assume that n longitudinal splitting cracks with equal length L in the range of $A \times L \times b$. The spacing of cracks is t.

From the energy equation $WD=SE+nW_s$ (Li 2007), the following equation is available.

$$\left(\frac{\sigma_y-\sigma_x}{2}\right)\varepsilon ALb=\left(\sigma_y{}^2+2\sigma_x{}^2-4\nu\sigma_y\sigma_x-2\nu\sigma_x^2\right)\frac{ALb}{2E}+\frac{\pi Eb^2t^4\sigma_t}{36L^3\sigma_{cr}}n \tag{6}$$

According to the Eq. (6), the number of cracks can be obtained. In the above formula, either $n=\frac{A}{t}-1$ or $n=\frac{A}{t}$ shows that the number of crack n has a relation with depth A.

In order to verify the correctness of the formula, the in-situ stress parameters and mechanical parameters of rock mass in underground powerhouse of the Ertan Hydropower Station were checked. Since after excavation unloading, $\sigma_y >> \sigma_x$, the influence of lateral force σ_x is neglected for simplicity. σ_y equals to the critical value σ'_{cr} when splitting crack occurs. For the underground powerhouse of the Ertan Hydropower Station, $A\approx 20$ m, $\sigma'_{cr}=0.2\sigma_f=30$ MPa, $\varepsilon_{cr}=2\times10^{-3}$, the length of crack L=5cm, longitudinal depth b=20 cm, the rock tensile strength σ_t = 5 MPa and the deformation modulus E= 30 GPa.

The Eq. (6) can be simplified as,

$$\frac{\sigma'_{cr}}{2}\varepsilon AL=\sigma'^2_{cr}\frac{AL}{2E}+\frac{b\sigma_t}{12\pi L}\mathrm{t}^2 n \tag{7}$$

If $\eta_1 = \frac{\sigma'_{cr}}{2}\varepsilon L$, $\eta_2 = \sigma'^2_{cr}\frac{L}{2E}$, $\eta_3 = \frac{b\sigma_t}{12\pi L}$, A is a constant, then there is the following the expression for A, n and t:

$$(\eta_1 - \eta_2)A = \eta_3 t^2 n \tag{8}$$

If the cracking depth and the average width between cracks are obtained by measuring, the number of crack can be estimated. According to these formulas, i.e. the number of crack $n = A/t$, the crack width $t = \frac{\eta_1 - \eta_2}{\eta_3}$, t equals to 0.72 m using the actual data, which is the minimum width and equivalent to approximately 28 cracks.

4. Numerical analysis of splitting failure by energy method

Based on the above analysis, the total energy (SD) of the entire rock comprises of (1) elastic strain energy (SE) (2) dissipated energy (W_s) due to crack propagation, i.e. $SD = SE + nW_s$. It is assumed that this energy is fully used for the energy dissipation of the formation of splitting cracks. The following method can be used to investigate the changes of the energy. In the numerical simulation, the appropriate strain-softening model is adopted for brittle rock (Wong *et al*. 2006). By tracking the whole process of the variation of elastic energy density of each unit, the energy difference of the unit before and after failure is recorded, i.e. $U_i = SD_i - SE_i$. Then the energy value of all the elements in the plastic zone is accumulated to obtain the total released energy (nW_s) of the surrounding rock, which is caused by the current excavation step.

In order to use numerical results, the definition of the calculation expression of energy for each unit is as follows:

(1) The elastic strain energy of the i-th unit before failure

$$SE_i = V_i\left[\left(\sigma_x^2 + \sigma_y^2 + \sigma_z^2\right) - 2\nu\left(\sigma_x\sigma_y + \sigma_x\sigma_z + \sigma_z\sigma_y\right)\right]/(2E) \tag{9}$$

(2) The elastic strain energy of the i-th unit during failure

$$SD_i = V_i\left[\left(\sigma^{*2}_x + \sigma^{*2}_y + \sigma^{*2}_z\right) - 2\bar{\nu}\left(\sigma_x^*\sigma_y^* + \sigma_x^*\sigma_z^* + \sigma_y^*\sigma_z^*\right)\right]/\left(2\bar{E}\right) \tag{10}$$

Where $\sigma_x, \sigma_y, \sigma_z$ are the main principal stresses of the unit before failure, $\sigma_x^*, \sigma_y^*, \sigma_z^*$ are the main principal stresses of the unit during failure. ν and E are Poisson's ratio and modulus of deformation respectively before the failure of the rock unit; $\bar{\nu}$ and $\bar{E}$ are Poisson's ratio and modulus of deformation respectively after the failure of the rock unit.

For simplicity, it is assumed that Poisson's ratio and modulus of deformation do not change before and after the failure.

Therefore, the change of energy generated within the failure region can be expressed as:

$$U = \sum_{i=1}^{n} SD_i - \sum_{i=1}^{n} SE_i \tag{11}$$

The above ideas reflect the energy dissipation of the surrounding rock of the entire failure region in the process of failure, by tracking the energy change per unit before and after failure. Thus the applicability of the energy method for analysis of rock failure can be examined.

5. Deflection analysis of thin plate

Considering the splitting surrounding rock at cavern sidewalls is equivalent to thin plate, the mechanical model can be simplified to the model simply supported at four edges. The curved surface equation, which takes the Fourier series as the critical state, conforms to the displacement boundary conditions (Altindag and Guney 2011). That is:

$$w = \sum_{m=1}^{\infty}\sum_{n=1}^{\infty} s\text{in}\frac{m\pi z}{L}\sin\frac{n\pi y}{b} \tag{12}$$

Where m is the number of half-wave for the plate deflection in the direction of the z-axis: n is the number of half-wave for the plate deflection in the direction of the y-axis.

When the thin plate changes from the stable equilibrium state of the plane to that of the slightly curved surface, the sum of the variation of the load potential energy and the strain energy in the thin plate is 0. (Altindag and Guney 2011) That is:

$$n\delta V + \delta U = 0 \tag{13}$$

Because of very small deflection that does not induce tension and compression in the neutral surface, it is acceptable to only consider bending and torsional deformation energy and potential energy changes of the force in the neutral plane, while ignoring the action of shear stress. Thus there are:

$$\delta V = \frac{D}{2}\int\int\left(\frac{\partial^2 w}{\partial z^2}+\frac{\partial^2 w}{\partial y^2}\right)^2 dzdy \tag{14}$$

$$\delta U = -\frac{t}{2}\int\int\left[\sigma_z\left(\frac{\partial w}{\partial z}\right)^2+\sigma_y\left(\frac{\partial w}{\partial y}\right)^2\right]dzdy \tag{15}$$

Put Eq. (12) into Eq. (14) ,

$$\delta V = \frac{LbD}{8}\sum_{m=1}^{\infty}\sum_{n=1}^{\infty}\left(\frac{m^2\pi^2}{L^2}+\frac{n^2\pi^2}{b^2}\right) \tag{16}$$

In order to obtain the maximum deflection, it should take m=1, n=1. Then δV can be expressed as

$$\delta V = \frac{LbD}{8}\left(\frac{\pi^2}{L^2}+\frac{\pi^2}{b^2}\right)^2 \tag{17}$$

By the theory of the thin plate deflection, the strain in the neutral surface is known. That is:

$$\left.\begin{aligned}\frac{1}{2}\left(\frac{\partial w}{\partial z}\right)^2 &= \varepsilon_z \\ \frac{1}{2}\left(\frac{\partial w}{\partial y}\right)^2 &= \varepsilon_y\end{aligned}\right\} \quad (18)$$

Using the energy method, the change of the potential energy of the force acting on the neutral surface (Wong *et al*. 2006) is:

$$\delta U = -tLb\sigma_z\left(\frac{1-\nu^2}{E}\sigma_z\right) - tLb\sigma_y\left(\frac{1-\nu^2}{E}\sigma_y\right) \quad (19)$$

From Eq. (12), the superimposed deflection value (ω) of thin rock plate under the stresses σ_z and σ_y can be obtained (pressure coefficient is λ, then $\sigma_z = \lambda\sigma_y$).

$$\omega = 4\sqrt{6}\frac{(1-\nu^2)L^2b^2(\lambda+1)\sigma_y}{nEt\pi^2(L^2+b^2)} \quad (20)$$

6. A case study: Ertan Hydropower Station

6.1 Engineering geological condition

The surrounding rock of the underground caverns in the Ertan Hydropower Station is fresh, Indosinian hard granite. The intact rock is hard. It belongs to the brittle rock material in the high in-situ stress zone, whose structural plane is weak without penetration.

The compressive strength of the rock is comparatively higher, which is 130.5 MPa. The tensile strength of the rock is relatively low, which is 6.24 MPa. The ratio between compressive and tensile strength of the rock is around 1/20. The deformation modulus E is between 30-50 GPa (details listed in Table 1). The underground caverns of the powerhouse are located in the high in-situ stress zone, which is mainly under the action of the tectonic stress, combined with the gravity stress.

Initial stress field: The difference of the stress magnitude and the azimuth in the rock mass is relatively small, i.e. σ1 = 21.1 ~ 27.3 MPa, the azimuth NE54° ~84°, which has little effect on the position of the underground powerhouses. The angle between NE45 ° and the maximum principal stress is 26.7°; the confining pressure ratio is 0.73, which is suitable for large underground caverns.

Table 1 The mechanical parameters of the rock for the Ertan Hydropower Station

Lithology	γ (kN/m^3)	E (GPa)	c (MPa)	σ_c (MPa)	σ_t (MPa)	μ	φ (°)
Granite	27.8	35	30	140	6.24	0.22	45

6.2 Main hydraulic structures

In the underground caverns of the Ertan Hydropower Station, there are three main chambers, namely, the main powerhouse, the main transformer room and the tail water surge chamber. They are arranged in parallel. The axial direction is N6E. The dimensions are as follows, the main house of that is 280.3 m × 25.5 m × 60.5 m (length × width × height); The main transformer room of that is 199.0 m × 17.4 m × 25.0 m (length × width × height); The tail water surge chamber of that is 203 m × 19.5 m × 58.1 m (length × width × height); The tail water chamber of that is 888.1 m × 16 m × 16 m (length × width × height).

The horizontal spacing of the main transformer room, the main building and the tail water surge chamber is 35 m and 30 m respectively. The entire underground powerhouse is located about 80m from the left shoulder of the arch dam. The average depth is 250 ~ 450 m and the lateral thickness of the rock is 300 m.

6.3 Numerical modelling

This chapter is mainly the qualitative analysis of energy changes in the process of cavern excavation. Therefore, to simplify the computational model, only the main powerhouse, the main transformer room and the tail water surge chamber are considered (see Fig. 2). Faults and other structural surfaces are not taken into account. The surrounding rock is taken as a single lithology temporarily.

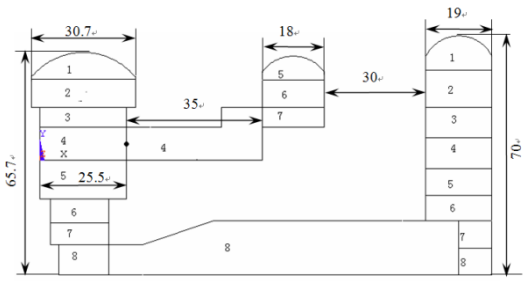

Fig. 2 The structural layout of Ertan underground powerhouse

The computational model takes the horizontal direction of the cross section of the powerhouse as the x axis and takes the vertical direction as the y axis. The longitudinal axis is the z axis. The range in x direction is from -333.05 m to - 482.35 m, where hydropower unit axis is the coordinate zero point; The range in y direction is from the elevation of 408.85 m to the ground surface. And the depth of the top of the chamber to the ground surface is 350 m. The quasi three dimensional model is adopted, that is to say, the plane model takes a certain thickness (b) along the axis of the powerhouse (b=20 m). The strain softening model embedded in FLAC (Song *et al.* 2015) is used to simulate the fracture zone of hard rock under high in-situ stresses.

6.4 Result analysis

Combined with the damage phenomenon of the Ertan Hydropower Station at site, in the numerical example, the 20 m deep rock column between the right side wall of the main powerhouse and the main transformer room was selected. To analyse the influence of excavation on the energy change of surrounding rock in different parts, 6 typical units were chosen and analysed, as shown in Fig. 3.

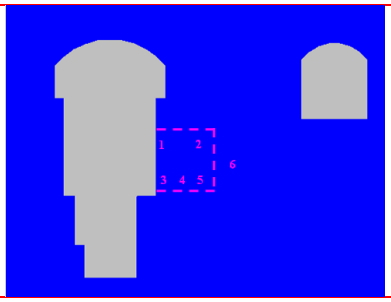

Fig. 3 The key units plan

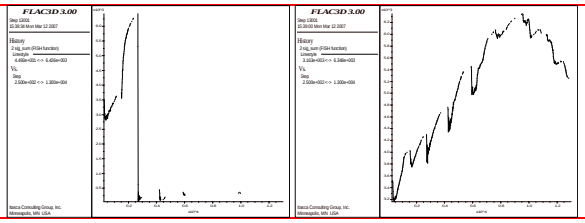

Fig. 4 The energy curve of unit 1&2 varying with the time-step

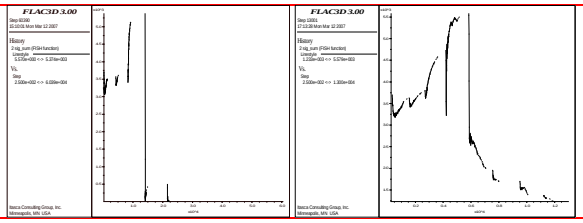

Fig. 5 The energy curve of unit 3&4 varying with the time-step

Unit 1 and unit 3 are the units in the vicinity of the side wall of the chamber. From Figs. 4-5, there are sudden energy drops of two units in the excavation process. The reason of sudden energy drops is that the radial stress in the surrounding rock released and greatly reduced due to excavation.

Although the tangential stress has a certain increase, in general the elastic energy is greatly reduced. The energy variables of the two units were 6280 J and 5349 J. As can be seen from the graph, the energy of the unit after a large stress drop tends to be stable basically with a little resilience, due to the smaller disturbance of the subsequent excavation step.

Unit 4 is a unit that is slightly far from the side wall of the main powerhouse than unit 1 and unit 3. It can be seen from Fig. 5 that this unit is also affected by the excavation of the cavern. It has a great change of energy as 3106 J. But compared to unit 1 and unit 3, the amount of change is smaller. It shows that the disturbance of excavation to the surrounding rock is gradually reduced with the increase of distance from the cavern. Unit 2 is farther from the wall compared to unit 4, and the excavation disturbance is small correspondingly. The energy change value is around 600 J.

Comparing the energy curves of unit 1, 2, 4 and those of unit 2 and 5, it can be found that the energy of unit 1, 2, 4 have a certain amount of growth for a period of time at the beginning, since stress change caused an increase in the elastic energy, dissipating some energy for crack propagation; The energy curves of unit 2, 5 gradually lift at the beginning. After the sudden energy drops, they decreased gradually. However, the ultimate energy value is higher than its initial energy value. It indicates that the energy of this section is still increased after excavation. In the meantime, if comparing the energy curves of unit 2 and 5, it can be found that the energy of unit 5 have reduced more. It explains that within the same distance to the side wall, the deeper the location, the easier it will crack and split, which agrees with the many experimental observations by other researchers (Hoek and Martin 2014, Ma and Haimson 2016, Huang *et al.* 2013).

Unit 6 is a point outside the selected region, which is in elastic state throughout the calculation. From Fig. 6, it indicates that the energy change has a growing trend. Each step of the excavation has little effect to this point. The maximum value is only about 100 J. Therefore, the excavation seems only affecting the area close to the cavern. This explains from the energy release side that why the splitting failure ranges is usually close to the excavation. It provides a new theoretical support to the splitting failure.

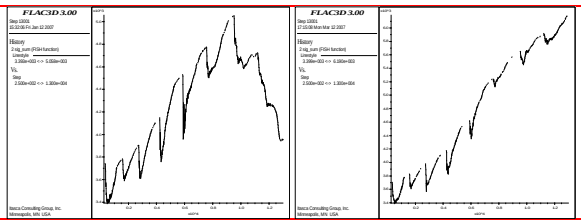

Fig. 6 The energy curve of unit 5&6 varying with the time-step

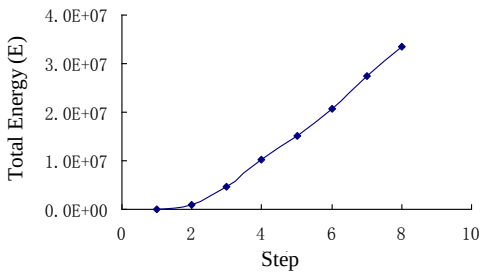

Fig. 7 Total energy dissipation change of the surrounding rock of the main powerhouse

The total energy of the selected area released after excavation is shown in Fig. 7 varying with the excavation step. It can be seen from Fig. 7, the release of energy increased gradually along with the excavation, generally close to the linear growth trend. After the eighth step excavation, the dissipation of energy can reach $\Delta U = 3.36e7$ J.

Based on the above formula of prediction of crack number which is according to the energy dissipation theory, the number of splitting cracks can be estimated in the selected area, $n = \Delta U / W_s$, where $W_s = \frac{\pi E b t^4 \sigma_t}{36 L^2 \sigma_{cr}}$, thus n = 26. According to the crack number obtained from Eq. (8), it is proved that the energy analysis method is used to predict the reliability of the split fracture. The crack number is close to that by formula 8. It is proved that the energy analysis method is reliable to predict the split cracks.

6.5 Prediction and analysis of splitting area and displacement

Splitting failure can be described as: after the excavation of underground caverns, the surrounding rock will appear stress concentration. This stress state is caused by excavation unloading of one side, leading to the compression state near the excavation area, as shown in Fig. 8 (a).

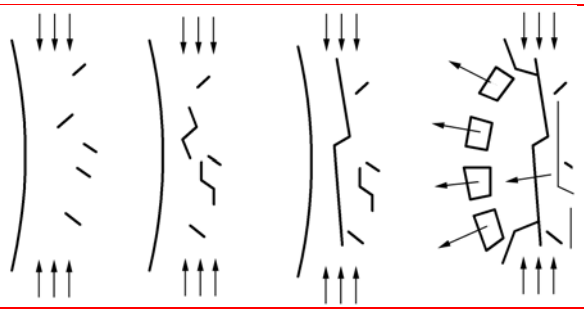

Fig. 8 Schematic diagrams of splitting failure of surrounding rock

Under further loading, the cracks expand as shown in Fig. 8 (b). It shows that, when cracks satisfy the condition K Imax $\geq K$ IC, they expand along the direction of maximum compressive stress in a stable manner.

As the load continues to increase, coupled with the influence of the free boundary and interaction between cracks, the crack propagation will no longer be stable. At this time the crack will grow suddenly, forming large run-through splitting cracks, as shown in Fig. 8 (c).

If the intensity is high enough, there will be more intense rock burst as shown in Fig. 8 (d). Therefore, cracking conditions can be defined as KImax $\geq K$ IC (Li 2014).

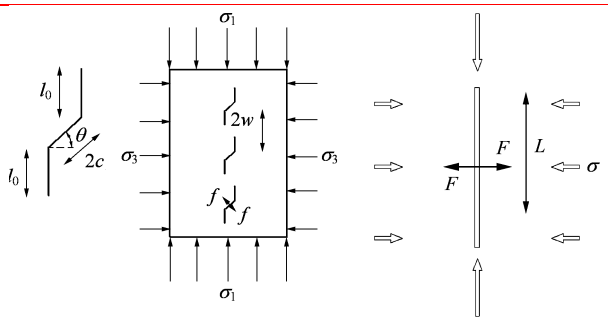

Fig. 9 Simplified model of splitting (Li 2014)

According to the mechanical model of Fig. 9, the criterion of splitting failure of rock mass is obtained (Li 2014):

The stress inequality after splitting failure is as follows:

$$\sigma_y \geqslant \frac{K_{IC}\sqrt{\pi L}}{L(\sin\theta\cos^2\theta - \mu\sin^2\theta\cos\theta)} + \sigma_x \frac{\pi + (\sin\theta\cos^2\theta + \mu\cos^3\theta)}{(\sin\theta\cos^2\theta - \mu\sin^2\theta\cos\theta)} \quad (21)$$

Where the initial crack length is $2c$, the crack length is $2l_0$, the adjacent crack spacing is $2w$, the initial crack surface and the angle between the horizontal direction is θ, the friction factor of the sliding surface is μ, the adjacent crack spacing is $2w$. When $l_0 = w$, cracks are connected to form a split crack, whose length is defined as L.

According to the engineering geological investigation report for the mechanical properties of the surrounding rock mass, combined with the analysis of Lajtai *et al.* (1991) for similar micro cracks in rock mass, and the use of the new parameters of the surrounding rock by feedback analysis, the micro crack parameters can be obtained by positive analysis (details listed in Table 2).

The crack angle θ should be more than 40 degrees, and the micro crack length is in millimetre scale. Considering the split spacing between micro cracks in the model is small, the length of the wing crack l_0 is suggested to be 1 to 3 times of the initial crack length. The initial crack density χ is determined by the integrity coefficient and Poisson's ratio of the surrounding rock (Martin *et al.* 2013).

Table 2 Micro crack parameters of granite for the Ertan Hydropower Station

θ (Angle of crack and horizontal stress) (°)	Friction coefficient (μ)	Initial crack length c (m)	Wing crack length l0 (m)	Initial crack density χ
45	0.50	0.002 5	0.005	0.024

The above mentioned parameters are brought into the splitting criterion i.e. Eq. (21) to get the splitting criterion related to this project,

$$\sigma_y \geqslant 4.09 + 20.40\sigma_x \quad (22)$$

The splitting failure criterion Eq. (22) was wrote into FISH language for FLAC 3D by Itasca Consulting Group Inc. (1997), which was applied into the excavation analysis of the Ertan Hydropower Station. The distribution map of the splitting failure area is obtained, as shown in Fig. 5 .The splitting failure zone of the main powerhouse was calculated to be about 16.2 m.

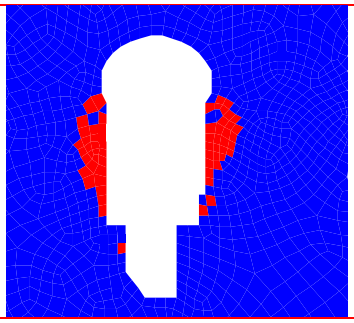

Fig. 10 Splitting failure zone of caverns after excavation

According to Fig. 10, for the surrounding rock of the right side wall of the main powerhouse, L = 19.32 m , b = 20 m. Based on the previous analysis, the maximum distance between the rock plates t is around 0.72 m, the number of splitting cracks is about 28, according to Eq. (20) it can be finally calculated that,

$$\omega = 4\sqrt{6}\frac{(1-\nu^2)L^2b^2(\lambda+1)\sigma_y}{nEt\pi^2(L^2+b^2)} = 37.75 \tag{23}$$

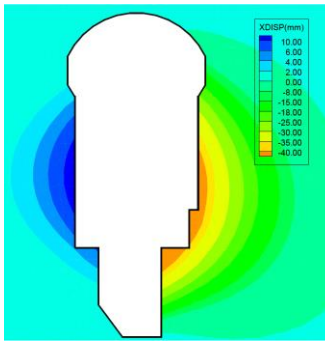

(a) Horizontal displacement of caverns

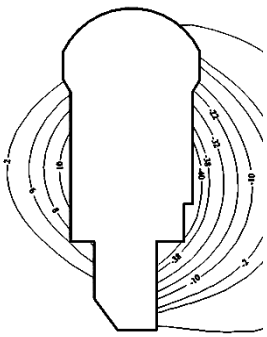

(b) The contour map

Fig. 11 Horizontal displacement of caverns and the contour map after excavation

Taking the main powerhouse for example, the displacement distribution in x direction and the contour map using FLAC 3D are shown in Fig. 11.

It can be seen from the Fig. 11 that the maximum displacement of X direction by numerical calculation is 38.5 mm, which is essentially consistent with the result of the analytical method. It provides that this method is reliable and accurate, so this method can provide a reliable calculation tool for similar project.

Besides, comparing the result of the numerical and analytical calculation, it can be found that the splitting failure ranges obtained by these two methods are close to each other. This further explains the correctness of the analytical method. Therefore, the analytical method proposed in this study can directly obtain the possible splitting failure range during excavation, which can then be a valuable reference for practical retaining design and stability monitoring.

7. Conclusions

Based on the theory of fracture mechanics to analyse the development of the splitting failure, and by applying the basic principle of energy dissipation, the total energy in the rock includes the elastic strain energy and the dissipated energy of the splitting crack formation. In addition, based on the thin plate buckling theory in elastic mechanics, the mechanism of instability and failure of rock pillar have been studied, and the critical load of rock pillar failure and the energy released by the buckling of thin plate are obtained. Therefore a failure criterion of splitting has been established. The criterion was used in numerical calculations, which helped to determine and directly show the splitting failure range of the underground powerhouses, for the purpose of retaining design and stability monitoring.

Combined with the conclusions above, and based on the thin plate theory in elastic mechanics, the generalized predictive formula to estimate the number of splitting cracks in damaged area was established. Furthermore, analytical formulas are derived respectively to calculate the critical stress and the maximum deflection of the thin plate under high in-situ stresses, causing the splitting failure of side wall of the brittle surrounding rock. Comparing to the numerical results of the underground powerhouses in the Ertan Hydropower Station, it shows that the method can be used to calculate the splitting failure with a good and consistent result.

So far, the mechanism of the splitting crack formation and the corresponding criteria has not been fully understood. There isn't a set of accurate calculation methods which can be accepted within the field of geotechnical engineering. Thus the determination methods and results of certain properties in this paper can be valuable references to the stability calculation of the splitting failure of the underground powerhouses, though with some errors.

Acknowledgments

We are grateful for the jointly support from the National Natural Science Foundation of China (Grant No. 41372294, 51579142 and 51779134). The research has greatly benefited from Program for Changjiang Scholars and Innovative Research Team in University of China (No.IRT13075), Opening Project Fund of State Key Laboratory of Mining Disaster Prevention and Control by Shandong Province and the Ministry of Science and Technology (No. MDPC201605) and China Scholarship Council.

References

Altindag, R., Guney, A. (2011), "Predicting the relationships between brittleness and mechanical properties (UCS, TS and SH) of rocks", *Int J Sci Res Essays*, **5**(16), 2107–2118.

Chatterjee, K., Choudhury, D., Rao, V.D. and Mukherjee, S.P. (2015), "Dynamic analyses and field observations on piles in kolkata city", *Geomech. Eng.*, **8**(3), 415–440.

Chinnasane, D.R. (2004), "Brittle rock rating for stability assessment of underground excavations", Ph.D. Dissertation, Laurentian University of Sudbury, Canada.

Hoek, E. and Martin, C.D. (2014), "Fracture initiation and propagation in intact rock—a review", *J Rock Mech Geotech Eng*, **6**(4), 287–300.

Hibino, S., Motojma, M. (1995), "Characteristic behavior of rock mass during excavation of large caverns", *Proceedings of the 8th International Congress on Rock Mechanics*, Tokyo, Japan, 583–586.

Huang, F., Zhu, H.H., Xu, Q.W., Cai, Y.C. and Zhuang, X.Y. (2013), "The effect of weak interlayer on the failure pattern of rock mass around tunnel – scaled model tests and numerical analysis", *Tunnelling and Underground Space Technology*, 35, 207–218.

Itasca Consulting Group Inc. (1997), *FLAC 3D manual*. USA, Itasca Consulting Group Inc.

Jiang, Q. and Feng, X.T. (2011), "Intelligent stability design of large underground hydraulic caverns", *Chinese method and practice. Energies*, **4**(10), 1542–1562.

Lajtai, E.Z., Carter, B.J. and Duncan, E.J.S. (1991), "Mapping the state of fracture around cavities", *Engineering Geology*, **31**, 277-289.

Li, X.J. (2007), "The study on experiment and theory of splitting failure in great depth openings", Ph.D. Dissertation, Shandong University, Jinan, China.

Li, X.J. (2014), "Displacement Forecasting Method in Brittle Crack Surrounding Rock under Excavation Unloading Incorporating Opening Deformation", *Rock Mechanics and Rock Engineering*, Volume **47**, Issue 6, 2211-2223.

Li, Y., Wang, H.P., Zhu, W.S., Li, S.C. and Liu J. (2015), "Structural stability monitoring of a physical model test on an underground cavern group during deep excavations using FBG sensors", *Sensors*, **15**(9), 21696–21709.

Li, Y., Zhu, W.S., Fu, J.W., Guo, Y.H. and Qi, Y.P. (2014), "A damage rheology model applied to analysis of splitting failure in underground caverns of Jinping I hydropower station", *International Journal of Rock Mechanics and Mining Sciences*, Volume **71**, Pages 224-234, ISSN 1365-1609, http://dx.doi.org/10.1016/j.ijrmms.2014.04.027.

Liolios, P. and Exadaktylos, G. (2013), "Comparison of a hyperbolic failure criterion with established failure criteria for cohesive-frictional materials", *Int J Rock Mech Min Sci*, **63**, 12–26.

Louchnikov, V. (2011), "Simple calibration of the extension strain criterion for its use in numerical modelling", *In: Potvin Y (ed) Strategic vs tactical approaches in mining. Australian Centre for Geomechanics*, Perth, 85–96.

Palchik, V. and Hatzor, Y.H. (2002), "Crack damage stress as a composite function of porosity and elastic matrix stiffness in dolomites and limestones", Eng Geol., **63**, 233–245.

Panaghi, K., Golshani, A. and Takemura, T. (2015), "Rock failure assessment based on crack density and anisotropy index variations during triaxial loading tests", *Geomech. Eng.*, **9**(6), 793–813.

Maheshwari, P. (2009), "Modified Stanley's approach for statistical analysis of compression strength test data of rock specimens", *Int J Rock Mech Min Sci*, **46**, 1154–1161.

Martin, C.D., Kaiser, P.K. and Christiansson, R. (2013), "Stress, instability and design of underground excavations", *Int J Rock Mech Min Sci*, **40**, 1027–1047.

Ma, X. and Haimson, B. (2016), Failure characteristics of two porous sandstones subjected to true triaxial stresses, *Journal of Geophysical Research-Solid Earth* **121** (9): 6477-6498

Ma, X., Rudnicki, J. and Haimson, B. (2017), Failure characteristics of two porous sandstones subjected to true triaxial stresses: applied through a novel loading path, *Journal of Geophysical Research-Solid Earth* **122** (4): 2525-2540

Ruffolo, R.M. and Shakoor, A. (2009), "Variability of unconfined compressive strength in relation to number of test samples", *Eng Geol*., **108**(1):16–23.

Sanchidrian, J.A., Ouchterlony, F., Moser, P., Segarra, P. and Lopez, L.M. (2012), "Performance of some distributions to describe rock fragmentation data", *Int J Rock Mech Min Sci.*, **53**, 18–31.

Song, D.Z., Wang, E.Y., Xu, J.K., Liu, X.F. and Shen, R.X. (2015), "Numerical simulation of pressure relief in hard coal seam by water jet cutting", *Geomech. Eng*., **8**(4), 495–510.

Sofianos, A.I., Nomikos, P.P. and Papantonopoulos, G. (2014), "Distribution of the factor of safety, in geotechnical engineering, for independent piecewise linear capacity and demand density functions", *Comput Geotech.*, **55**, 440–447.

Tang, C.A., Lin, P., Wong, R.H.C. and Chau, K. T. (2004), "Analysis of crack coalescence in rock-like materials containing three flaws-Part Ⅱ:numerical approach", *International Journal of Rock Mechanics and Mining Sciences*, **38**(7), 925-939.

Wang, H.P., Li, Y., Li, S.C., Zhang, Q.S. and Liu, J. (2016), "An elasto-plastic damage constitutive model for jointed rock mass with an application", *Geomech. Eng.*, **11**(1), 77–94.

Wong, L.N.Y. and Einstein, H.H. (2009), "Crack coalescence in molded gypsum and Carrara marble: part 1. Macroscopic observation sand interpretation", *Rock Mech Rock Eng*., **42**(3), 475–511.

Wong, T.F., Wong, R.H.C., Chau K.T. and Tang, C.A. (2006), "Microcrack statistics, Weibull distribution and micromechanical modeling of compressive failure in rock", *Mech Mater.*, **38**, 664–681.

Wu, Z., and Wong, L.N.Y. (2012), "Frictional crack initiation and propagation analysis by numerical manifold method", *Comput Geotech*. **39**(1), 38–53.

Xue, X.H. (2015), "Study on relations between porosity and damage in fractured rock mass", *Geomech. Eng.*, **9**(1), 15–24.

Zhu, W.S., Yang, W.M., Li X.J., Xiang L., and Yu D.J. (2014), "Study on splitting failure in rock masses by simulation test, site monitoring and energy model", *Tunnelling and Underground Space Technology*, Volume **41**, Pages 152-164, ISSN 0886-7798, http://dx.doi.org/10.1016/j.tust.2013.12.007.